ARTICLE

Beneficial metabolic effects of M_3 muscarinic acetylcholine receptor deficiency

Dinesh Gautam,[1] Oksana Gavrilova,[2] Jongrye Jeon,[1] Stephanie Pack,[2] William Jou,[2] Yinghong Cui,[1] Jian H. Li,[1] and Jürgen Wess[1,*]

[1] Molecular Signaling Section, Laboratory of Bioorganic Chemistry
[2] Mouse Metabolic Core Laboratory
National Institute of Diabetes and Digestive and Kidney Diseases, Bethesda, Maryland 20892
*Correspondence: jwess@helix.nih.gov

Summary

Most animal models of obesity and hyperinsulinemia are associated with increased vagal cholinergic activity. The M_3 muscarinic acetylcholine receptor subtype is widely expressed in the brain and peripheral tissues and plays a key role in mediating the physiological effects of vagal activation. Here, we tested the hypothesis that the absence of M_3 receptors in mice might protect against various forms of experimentally or genetically induced obesity and obesity-associated metabolic deficits. In all cases, the lack of M_3 receptors greatly ameliorated impairments in glucose homeostasis and insulin sensitivity but had less robust effects on overall adiposity. Under all experimental conditions tested, M_3 receptor-deficient mice showed a significant elevation in basal and total energy expenditure, most likely due to enhanced central sympathetic outflow and increased rate of fatty-acid oxidation. These findings suggest that the M_3 receptor may represent a potential pharmacologic target for the treatment of obesity and associated metabolic disorders.

Introduction

Obesity and obesity-associated type 2 diabetes have emerged as two of the major threats to human health in the 21st century (Yach et al., 2006). As a result, the molecular pathways regulating appetite and fat storage have become the subject of intense investigation. Several lines of evidence indicate that central and peripheral cholinergic pathways play an important role in the regulation of glucose and energy homeostasis (Bray and York, 1979; Niijima, 1989; Rohner-Jeanrenaud, 1995; Ahren, 2000; Gilon and Henquin, 2001; Lam et al., 2005). Interestingly, most animal models of obesity and hyperinsulinemia are associated with increased vagal cholinergic activity and reduced sympathetic tone (Rohner-Jeanrenaud, 1995; Gilon and Henquin, 2001). Increases in the tone of peripheral parasympathetic (vagal) nerves leads to enhanced acetylcholine release, triggering changes in the activity of various effector organs and tissues involved in the regulation of glucose and energy homeostasis (Niijima, 1989; Ahren, 2000; Gilon and Henquin, 2001).

The physiological actions of acetylcholine released from parasympathetic nerve endings are mediated by a family of G protein-coupled receptors referred to as muscarinic acetylcholine receptors (Wess, 1996; Caulfield and Birdsall, 1998). Molecular cloning studies have revealed the existence of five different muscarinic receptor subtypes (M_1–M_5) (Wess, 1996; Caulfield and Birdsall, 1998). The M_3 muscarinic receptor subtype is widely expressed throughout the brain and in many peripheral organs (Levey et al., 1994; Eglen et al., 1996; Wess, 1996; Caulfield and Birdsall, 1998; Yamada et al., 2001) and mediates many of the physiological effects of vagal activation (Eglen et al., 1996; Wess, 1996; Caulfield and Birdsall, 1998).

In this study, we tested the hypothesis that the absence of M_3 receptors might protect against different forms of experimentally and genetically induced obesity and the associated metabolic deficits. This work was prompted by our previous observation that M_3 muscarinic receptor-deficient mice ($M3R^{-/-}$ mice) showed reduced adiposity when maintained on regular mouse chow (Yamada et al., 2001). In order to induce obesity, glucose intolerance, and insulin resistance, mice were maintained on a high-fat diet or were treated with gold-thioglucose (GTG), which induces hyperphagia by selectively destroying glucose-receptive neurons in the ventromedial nucleus of the hypothalamus (Bergen et al., 1998). In addition, we also examined whether the lack of M_3 receptors was able to prevent the increase in body weight and the metabolic complications caused by the absence of leptin. To address this issue, we generated and analyzed mutant mice that were deficient in both leptin and M_3 receptors ($M3R^{-/-}$ *ob/ob* mice).

In all three experimental models of obesity, $M3R^{-/-}$ mice were largely protected against obesity-associated glucose intolerance, insulin resistance, hyperinsulinemia, and hyperglycemia. Our data suggest that enhanced energy expenditure caused by the absence of M_3 muscarinic receptors represents a major factor contributing to these findings.

Results

All studies were carried out with male $M3R^{+/+}$ and $M3R^{-/-}$ mice (littermates) that had been backcrossed for 10 generations onto the C57BL/6NTac background.

The absence of M_3 receptors protects against diet-induced obesity and associated metabolic deficits

The consumption of an energy-rich, high-fat diet is known to trigger obesity and various metabolic changes including impaired glucose tolerance, insulin resistance, and hyperglycemia.

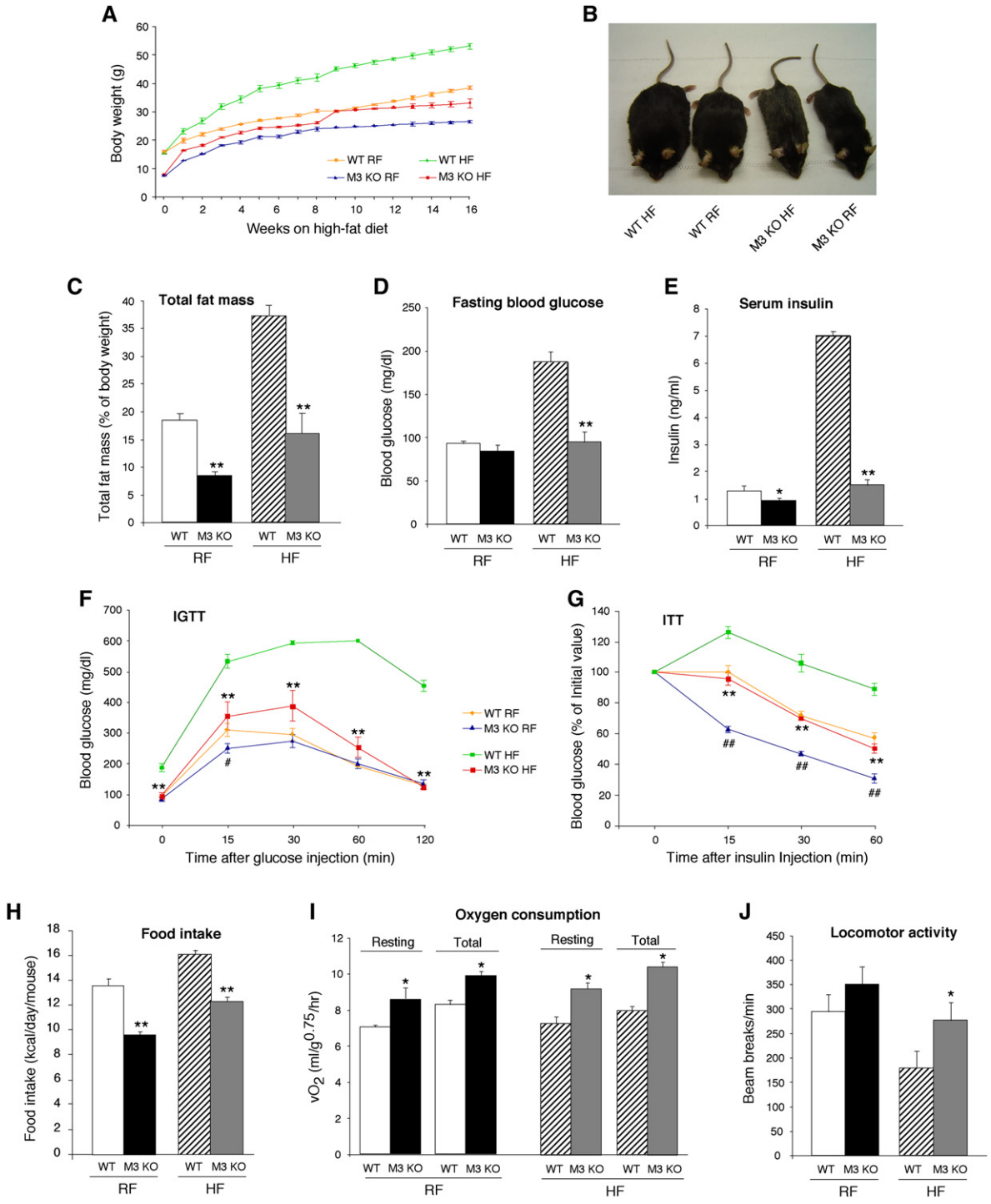

Figure 1. Analysis of male M3R$^{+/+}$ and M3R$^{-/-}$ mice maintained on a high-fat diet, as compared to mice consuming regular mouse chow

A) Growth curves. At all time points, M3R$^{-/-}$ mice (M3 KO) weighed significantly less than their M3R$^{+/+}$ (WT) littermates (HF, high-fat diet; RF, regular mouse chow; $p < 0.01$). **B)** Physical appearance of 9-month-old mice. **C)** Total body fat mass (% of body weight; 5-month-old males). **D)** Fasting blood glucose levels (14-week-old males). **E)** Serum insulin levels (freely fed 14-week-old males). **F)** Intraperitoneal glucose tolerance test (4-month-old males). **G)** Insulin tolerance test (4.5-month-old males). **H)** Food intake (Kcal/day/mouse; 10-month-old males). **I)** Resting and total metabolic rate (O_2 consumption; 5-month-old males). **J)** Locomotor activity (beam breaks per min; 5-month-old males). Data are given as means ± SEM (n = 6–9 per group). *$p < 0.05$; **$p < 0.01$ (panels **F** and **G**: *$p < 0.05$; **$p < 0.01$, as compared to the corresponding WT HF group; $^{\#}p < 0.05$; $^{\#\#}p < 0.01$, as compared to the corresponding WT RF group). vO_2, volume of O_2 consumed.

To investigate whether deletion of the M_3 receptor gene could prevent or reduce the severity of these metabolic deficits, 4-week-old M3R$^{+/+}$ and M3R$^{-/-}$ mice were fed a high-fat diet (fat content: 35.5%, w/w) and then monitored for 16 weeks. Mice consuming regular chow (fat content: 5%, w/w) were analyzed in parallel for control purposes.

M3R$^{-/-}$ mice maintained on regular chow showed a significant reduction in body weight and total body fat, reduced serum

Table 1. Body weight, plasma leptin levels, body composition, and body temperature of $M3R^{-/-}$ mice and control littermates under different experimental conditions

Genotype	Food	Treatment	N	Body weight (g)	Plasma leptin (ng/ml)	% Fat	% Lean mass	Body temp. (°C)
Group I								
$M3R^{+/+}$	RF	—	7	32.1 ± 0.8	11.0 ± 0.4	17.6 ± 1.9	72.9 ± 1.5	36.2 ± 0.2
$M3R^{-/-}$	RF	—	6	25.9 ± 0.7**	6.3 ± 0.5**	8.0 ± 1.1**	78.7 ± 1.1**	37.3 ± 0.2*
$M3R^{+/+}$	HF	—	7	43.0 ± 1.9	25.6 ± 2.8	35.7 ± 1.6	60.3 ± 1.2	36.3 ± 0.2
$M3R^{-/-}$	HF	—	8	30.9 ± 1.5**	10.8 ± 2.2**	16.0 ± 3.7**	74.0 ± 3.4**	37.2 ± 0.2*
Group II								
$M3R^{+/+}$	RF	Saline	13	35.6 ± 1.5	14.5 ± 1.6	24.6 ± 3.2	68.5 ± 2.4	35.2 ± 0.2
$M3R^{-/-}$	RF	Saline	7	29.6 ± 1.8**	7.0 ± 1.4**	9.0 ± 1.6**	77.5 ± 1.1**	36.1 ± 0.1*
$M3R^{+/+}$	RF	GTG	5	53.6 ± 2.2	32.7 ± 1.0	41.9 ± 2.3	55.4 ± 1.7	35.5 ± 0.2
$M3R^{-/-}$	RF	GTG	7	31.8 ± 2.0**	12.8 ± 2.5**	26.6 ± 4.0**	66.6 ± 2.9**	36.2 ± 0.1*
Group III								
$M3R^{+/+}$	RF	—	10	33.0 ± 1.0	ND	18.0 ± 2.5	73.6 ± 2.0	37.1 ± 0.1
$M3R^{-/-}$	RF	—	9	24.0 ± 0.6**	ND	8.0 ± 0.6**	79.7 ± 0.5**	37.8 ± 0.4*
ob/ob $M3R^{+/+}$	RF	—	12	66.2 ± 1.1	ND	53.0 ± 0.7	48.1 ± 0.5	36.2 ± 0.2
ob/ob $M3R^{-/-}$	RF	—	8	40.9 ± 1.6**	ND	48.8 ± 0.7**	50.7 ± 0.6**	36.6 ± 0.2*

Except for the leptin measurements which were carried out with 6-month-old mice, all measurements were carried out with 5-month-old male littermates. Data are expressed as means ± SEM. RF, regular mouse chow; HF, high-fat diet; ND, not determined because *ob/ob* mice are leptin-deficient. *$P<0.05$, **$P<0.01$, as compared to the corresponding control ($M3R^{+/+}$) group.

insulin levels, and increased glucose tolerance and insulin sensitivity (Figures 1A–1G), as compared to their $M3R^{+/+}$ littermates (also see Yamada et al., 2001; Duttaroy et al., 2004). In $M3R^{+/+}$ mice, consumption of the high-fat diet led to pronounced weight gain, hyperglycemia, hyperinsulinemia, impaired glucose tolerance, and insulin resistance (Figures 1A–1G; Table 1). Strikingly, these metabolic deficits induced by the consumption of the high-fat diet were largely absent in $M3R^{-/-}$ mice (Figures 1A–1G; Table 1).

In general, plasma leptin levels (Table 1) and body mass index (BMI) measurements (Table S1 available with this article online) correlated well with whole body adiposity (% fat; Table 1). Body length (nose to anus) measurements showed that $M3R^{-/-}$ mice maintained on either regular chow or the high-fat diet were somewhat smaller (by ~3–5 mm, corresponding to a ~3%–5% reduction in body length) than their corresponding $M3R^{+/+}$ littermates (Table S1), indicating that reduced body size also contributes to the decrease in body weight displayed by the $M3R^{-/-}$ mice.

$M3R^{-/-}$ mice maintained on regular chow or on the high-fat diet consumed significantly less food than their $M3R^{+/+}$ littermates (Figure 1H). Independent of the type of diet that the mice consumed, $M3R^{-/-}$ mice showed significantly increased rates of resting and total energy expenditure (measured as rate of O_2 consumption over 24 hr) and locomotor activity (Figures 1I and 1J). There were no significant differences in respiratory exchange ratios (RERs; ratio of CO_2 produced to O_2 consumed) among the $M3R^{+/+}$ and $M3R^{-/-}$ groups maintained on regular chow (data not shown). Interestingly, when consuming the high-fat diet, the $M3R^{-/-}$ mice showed a significantly lower RER than the control littermates (0.71 ± 0.01 ± versus 0.78 ± 0.01, $p < 0.0001$; n = 7 per group; 5-month-old males), suggesting increased fatty-acid oxidation. We also noted that the core body temperature was ~1°C higher in $M3R^{-/-}$ than in $M3R^{+/+}$ mice, independent of whether mice consumed regular chow or the high-fat diet (Table 1). This increase in body temperature was not only seen during the light phase (1–3 p.m.; Table 1) but also at midnight during the dark phase ($M3R^{+/+}$, 36.5°C ± 0.1°C, n = 13; $M3R^{-/-}$, 37.0°C ± 0.1°C, n = 16; $p < 0.01$; 6-month-old males maintained on regular chow). Similarly, the diurnal pattern of changes in locomotor activity remained intact in $M3R^{-/-}$ mice (Figure S1).

To exclude the possibility that the lack of M_3 receptors interfered with the breakdown or absorption of fat from the gastrointestinal tract, we used a technique recently developed by Jandacek et al. (2004). This method involves the inclusion of sucrose polybehenate (olestra) as an internal nonabsorbable marker in a high-fat diet (fat content: 35.5%, w/w) primarily consisting of safflower oil. This analysis showed that $M3R^{-/-}$ mice were able to absorb dietary fat equally well as their $M3R^{+/+}$ littermates (% fat absorption: $M3R^{+/+}$, 98.2% ± 0.3%; $M3R^{-/-}$, 96.1% ± 1.2%; n = 6 per group; 16-week-old males). Moreover, to exclude the possibility that food malabsorption caused by impaired gastrointestinal motility contributed to the reduced body weight displayed by the $M3R^{-/-}$ mice, we carried out a charcoal transit test to monitor gastrointestinal motor function in vivo. In this test, gastrointestinal transit of an intragastrically administered charcoal suspension is expressed as the ratio between the distance traveled by the charcoal during the 20 min period after administration and the total length of the small intestine. We found that the lack of M_3 receptors had no significant effect on gastrointestinal motility in vivo ($M3R^{+/+}$, 0.53 ± 0.03; $M3R^{-/-}$, 0.53 ± 0.03; n = 10 per group; 8.5-month-old males).

We carried out additional metabolic studies with relatively young $M3R^{+/+}$ and $M3R^{-/-}$ mice maintained on regular chow (mouse age: ~7 weeks). The young $M3R^{-/-}$ mice showed reduced food intake and body weight but did not differ from control mice in whole-body adiposity (% fat per body weight), glucose tolerance, insulin sensitivity, and several other metabolic parameters (Figure S2; Table S2), indicating that the phenotypic changes observed with adult $M3R^{-/-}$ mice require several months to develop. These data also suggest that the increase in glucose tolerance and insulin sensitivity displayed by the adult $M3R^{-/-}$ mice may be at least partially due to reduced adiposity.

The lack of M_3 receptors prevents GTG-induced obesity and associated metabolic deficits

The hypothalamus represents the main central regulator of energy homeostasis, food intake, and body weight. Classical

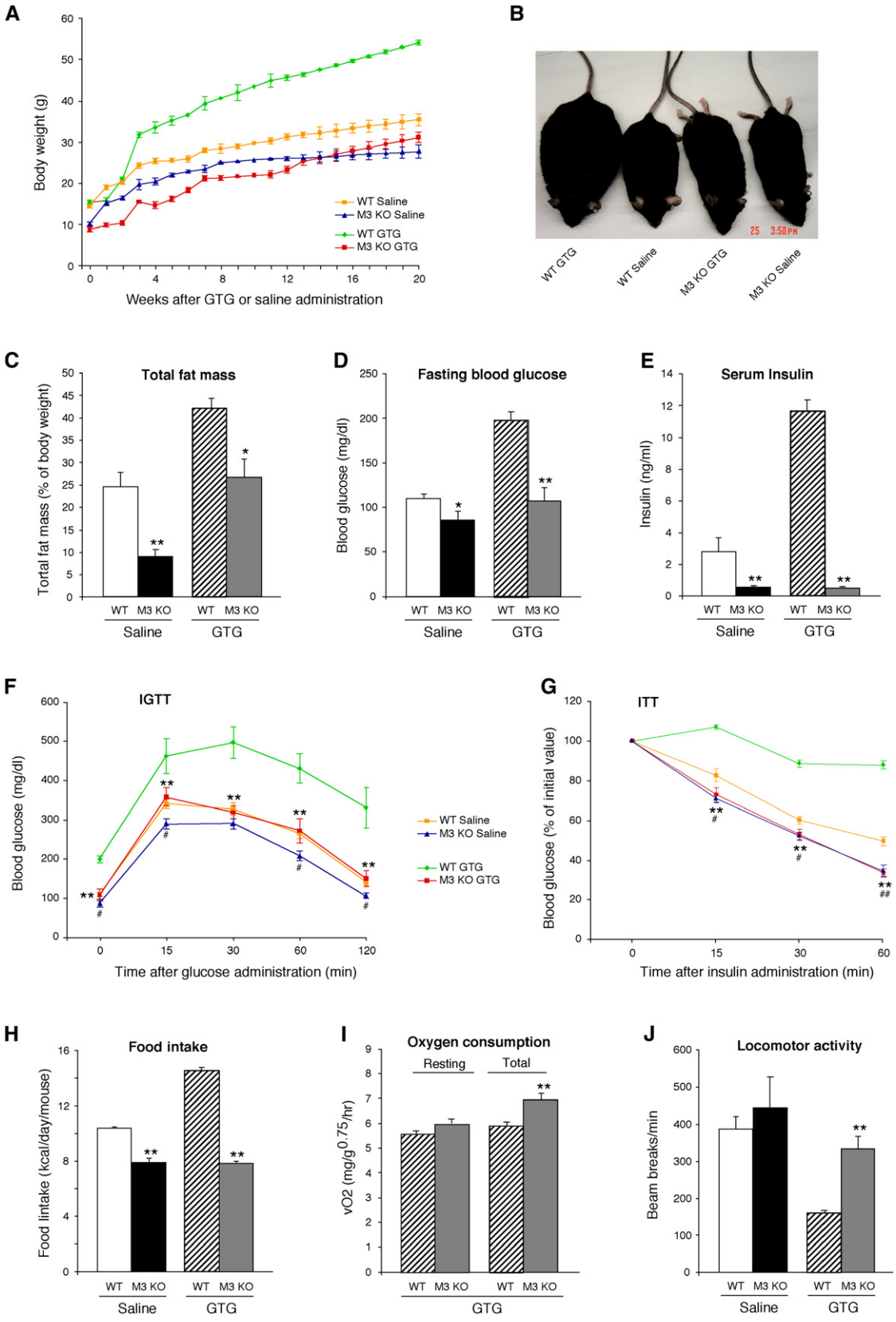

Figure 2. Analysis of M3R$^{+/+}$ and M3R$^{-/-}$ mice treated with a single dose of GTG or saline at 4 weeks of age

All experiments were carried out with male mice maintained on regular mouse chow. **A)** Growth curves. At all time points, M3R$^{-/-}$ mice (M3 KO) weighed significantly less than their M3R$^{+/+}$ (WT) littermates (GTG or saline treatment; $p < 0.01$). **B)** Physical appearance of 9-month-old mice. **C)** Total body fat mass (% of body weight; 5-month-old males). **D)** Fasting blood glucose levels (10-week-old males). **E)** Serum insulin levels (freely fed 10-week-old males). **F)** Intraperitoneal glucose tolerance test (4-month-old

studies of animals with hypothalamic lesions indicate the existence of a satiety center in the ventromedial hypothalamic nucleus (VMH) (Schwartz et al., 2000). Administration of gold-thioglucose (GTG) is known to trigger the selective ablation of neurons in the VMH, resulting in hyperphagia, obesity, insulin resistance, and glucose intolerance (Bergen et al., 1998).

To examine whether the lack of M_3 receptors protected against GTG-induced obesity and the associated metabolic deficits, 4-week-old $M3R^{+/+}$ and $M3R^{-/-}$ mice received a single i.p. injection of GTG (0.5 mg/g; Röhl et al., 2004). As shown in Figures 2A and 2B, GTG-treated $M3R^{+/+}$ mice gained significantly more weight than saline-treated mice of the same genotype. This increase in body weight was associated with a pronounced increase in body fat mass, hyperglycemia, and hyperinsulinemia (Figures 2C–2E; Table 1). Moreover, GTG-treated $M3R^{+/+}$ mice developed glucose intolerance and insulin resistance, as shown in i.p. glucose and insulin tolerance tests, respectively (Figures 2F and 2G).

In striking contrast, GTG-treated $M3R^{-/-}$ mice did not gain significantly more body weight than their saline-treated $M3R^{-/-}$ littermates (Figures 2A and 2B; Table 1) and had ~35%–40% less body fat than the GTG-treated $M3R^{+/+}$ mice (Figure 2C; Table 1). Moreover, GTG-treated $M3R^{-/-}$ mice showed similar blood glucose and serum insulin levels, glucose tolerance, and insulin sensitivity as saline-treated littermates of the same genotype (Figures 2D–2G). Plasma leptin levels correlated well with whole-body adiposity (% fat; Table 1).

In $M3R^{+/+}$ mice, GTG treatment led to an increase in food intake, decreased metabolic rate (data not shown), and reduced locomotor activity, as compared to saline-treated $M3R^{+/+}$ littermates ($p < 0.01$; Figures 2H and 2J). In contrast, GTG-treated $M3R^{-/-}$ mice showed significantly reduced food intake, elevated metabolic rate (resting and total), and increased locomotor activity, as compared to GTG-treated $M3R^{+/+}$ mice (Figures 2H–2J). RERs did not differ significantly between the $M3R^{+/+}$ and $M3R^{-/-}$ groups (data not shown). The core body temperature of $M3R^{-/-}$ mice was ~0.7°C–0.9°C higher than that of $M3R^{+/+}$ mice, independent of whether mice were treated with saline or GTG (Table 1).

Generation and analysis of mutant mice deficient in both M_3 receptors and leptin

Loss of leptin signaling in *ob/ob* mice causes severe obesity, hyperglycemia, and insulin resistance, as a result of improper regulation of food intake and energy expenditure (Schwartz et al., 2000). To examine whether lack of M_3 receptors affected the metabolic deficits displayed by *ob/ob* mice, we generated and analyzed $M3R^{-/-}$ *ob/ob* mice that were deficient in both M_3 receptors and leptin.

In comparison to wild-type littermates, *ob/ob* mice showed a striking increase in body weight and total body fat mass, significantly increased blood glucose and insulin levels, impaired glucose tolerance, and reduced insulin sensitivity (Figures 3A–3G; Table 1). Moreover, as compared to wild-type littermates, *ob/ob* mice exhibited a pronounced increase in food intake, decreased metabolic rate (data not shown), and a significant reduction in locomotor activity ($p < 0.01$; Figures 3H and 3J).

$M3R^{-/-}$ *ob/ob* mice showed a strikingly different phenotype. Although these mutant animals still exhibited a high degree of adiposity (compared to *ob/ob* mice), they displayed significantly decreased blood glucose and insulin levels and normal (wild-type-like) glucose tolerance and insulin sensitivity (Figures 3C–3G; Table 1). In addition, $M3R^{-/-}$ *ob/ob* mice consumed significantly less food and showed an increase in metabolic rate (resting and total) and locomotor activity, as compared to *ob/ob* mice (Figures 3H–3J). The absence of M_3 receptors had no significant effect on RERs (data not shown). The core body temperature of $M3R^{-/-}$ *ob/ob* mice was ~0.4°C higher than that of *ob/ob* mice (Table 1).

Thyroid hormone and free fatty-acid levels of $M3R^{+/+}$ and $M3R^{-/-}$ mice

Since elevated levels of thyroid hormones are known to lead to increased metabolic rate, body temperature, and locomotor activity, we measured circulating T3 and T4 levels in $M3R^{+/+}$ and $M3R^{-/-}$ mice maintained on regular chow. We found that the lack of M_3 receptors did not lead to increased plasma T3 and T4 levels (T3: $M3R^{+/+}$, 90.3 ± 2.1 ng/dl; $M3R^{-/-}$, 77.5 ± 1.5 ng/dl; T4: $M3R^{+/+}$, 3.6 ± 0.2 μg/dl; $M3R^{-/-}$, 3.4 ± 0.1 μg/dl; 5-month-old males; n = 5–8 per group). In fact, T3 levels were ~15% lower in $M3R^{-/-}$ mice than in wild-type littermates ($p < 0.01$).

Plasma-free fatty-acid levels tended to be higher in $M3R^{-/-}$ than in $M3R^{+/+}$ mice ($M3R^{+/+}$, 0.44 ± 0.04 mM; $M3R^{-/-}$, 0.50 ± 0.03 mM; 5-month-old freely fed males; n = 8 per group). However, this difference failed to reach statistical significance ($p = 0.17$).

Increased excretion of epinephrine and norepinephrine in the urine of $M3R^{-/-}$ mice

Many of the phenotypic changes displayed by the $M3R^{-/-}$ mice, including the observed increases in metabolic rate, body temperature, and locomotor activity, are reminiscent of the effects associated with an increased activity of the sympathetic nervous system (SNS; Hoffman and Taylor, 2001). To assess whether SNS activity was increased in the absence of M_3 receptors, we determined epinephrine and norepinephrine levels in the urines of $M3R^{+/+}$ and $M3R^{-/-}$ mice. Urine samples were collected over a 24 hr period in awake, freely moving animals. We found that the daily excretion of epinephrine and norepinephrine was significantly increased in $M3R^{-/-}$ mice ($p < 0.05$), indicative of increased SNS activity (epinephrine in ng/g body weight/24 hr: $M3R^{+/+}$, 4.6 ± 1.2; $M3R^{-/-}$, 9.7 ± 1.6; norepinephrine in ng/g body weight/24 hr: $M3R^{+/+}$, 38.4 ± 6.0; $M3R^{-/-}$, 55.7 ± 3.6; 6-month-old males; n = 12 per group).

Skeletal muscle, liver, and fat tissue do not express detectable amounts of M_3 muscarinic receptor protein

M_3 muscarinic receptors are known to be expressed in smooth muscle and glandular tissues and in most regions of the CNS (Levey et al., 1994; Wess, 1996; Caulfield and Birdsall, 1998). Since $M3R^{-/-}$ mice showed pronounced metabolic changes, we examined whether M_3 receptors were also expressed by

males). **G)** Insulin tolerance test (5-month-old males). **H)** Food intake (Kcal/day/mouse; 3.5-month-old males). **I)** Resting and total metabolic rate (O_2 consumption; 5-month-old males). **J)** Locomotor activity (beam breaks per min; 5-month-old males). Data are given as means ± SEM (WT-saline, n = 10–13; KO-saline, n = 7 or 8; WT GTG, n = 5; KO GTG, n = 7–10). *$p < 0.05$; **$p < 0.01$ (panels **F** and **G**: *$p < 0.05$; **$p < 0.01$, as compared to the corresponding WT GTG group; #$p < 0.05$; ##$p < 0.01$, as compared to the corresponding WT saline group). vO_2, volume of O_2 consumed.

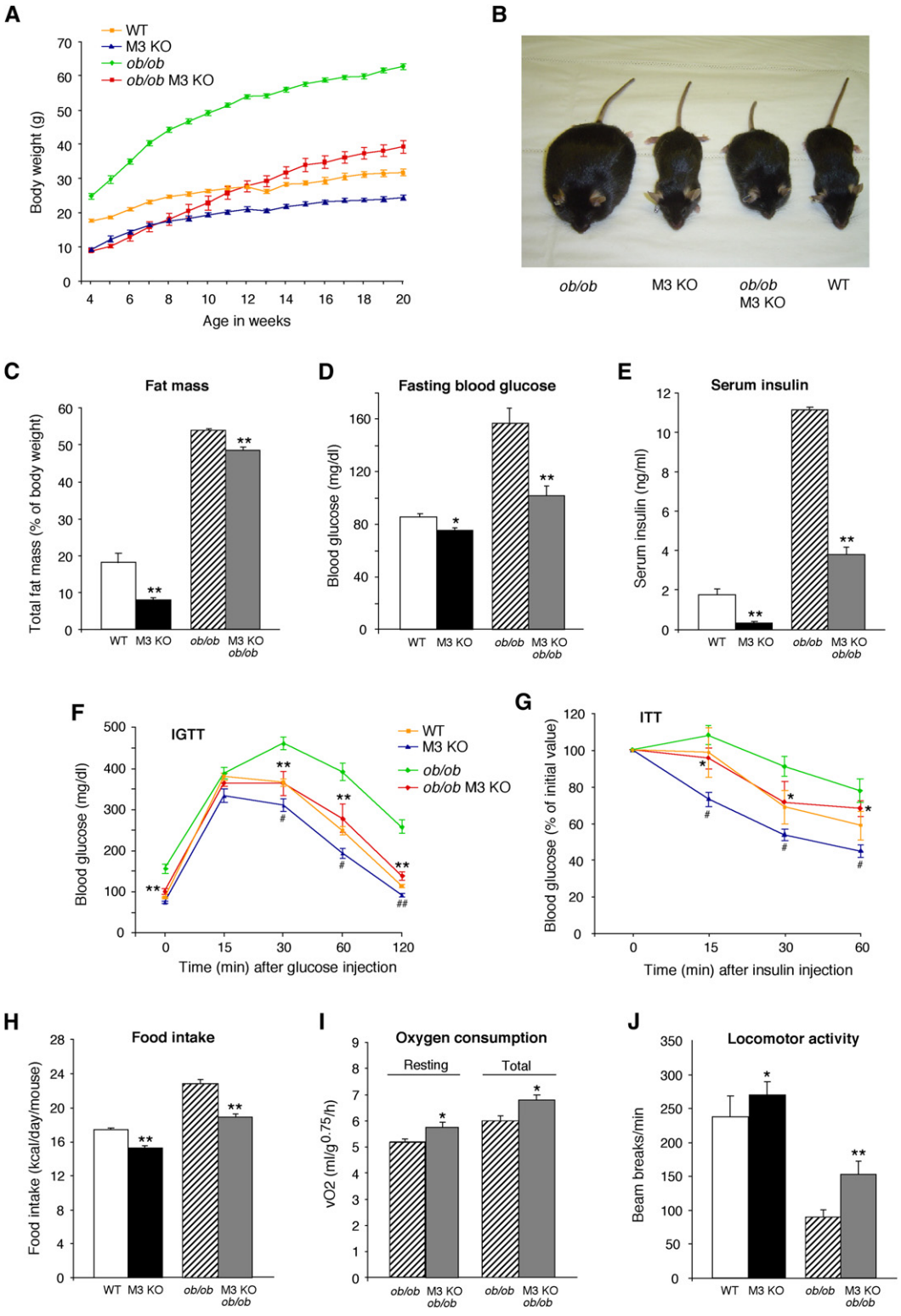

Figure 3. Analysis of *ob/ob* mice and M3R$^{-/-}$ *ob/ob* double knockout mice

For control purposes, M3R$^{+/+}$ (WT) and M3R$^{-/-}$ mice (M3 KO) were studied in parallel. All experiments were carried out with male mice maintained on regular mouse chow. **A)** Growth curves. At all time points, M3R$^{-/-}$ *ob/ob* double knockout mice (*ob/ob* M3 KO) weighed significantly less than *ob/ob* littermates ($p < 0.01$). **B)** Physical appearance of 6-month-old mice. **C)** Total body fat mass (% of body weight; 5-month-old males). **D)** Fasting blood glucose levels (14-week-old males). **E)** Serum insulin levels (freely fed 14-week-old males). **F)** Intraperitoneal glucose tolerance test (4.5-month-old males). **G)** Insulin tolerance test (4.5-month-old males). **H)** Food intake (Kcal/day/mouse; 3.5-month-old males). **I)** Resting and total metabolic rate (O_2 consumption; 5-month-old males). **J)** Locomotor activity (beam breaks per min; 5-month-old males). Data are given as means ± SEM (n = 5–12 per group). *$p < 0.05$; **$p < 0.01$ (panels **F** and **G**: *$p < 0.05$; **$p < 0.01$, as compared to the corresponding *ob/ob* group; #$p < 0.05$; ##$p < 0.01$, as compared to the corresponding WT group). vO_2, volume of O_2 consumed.

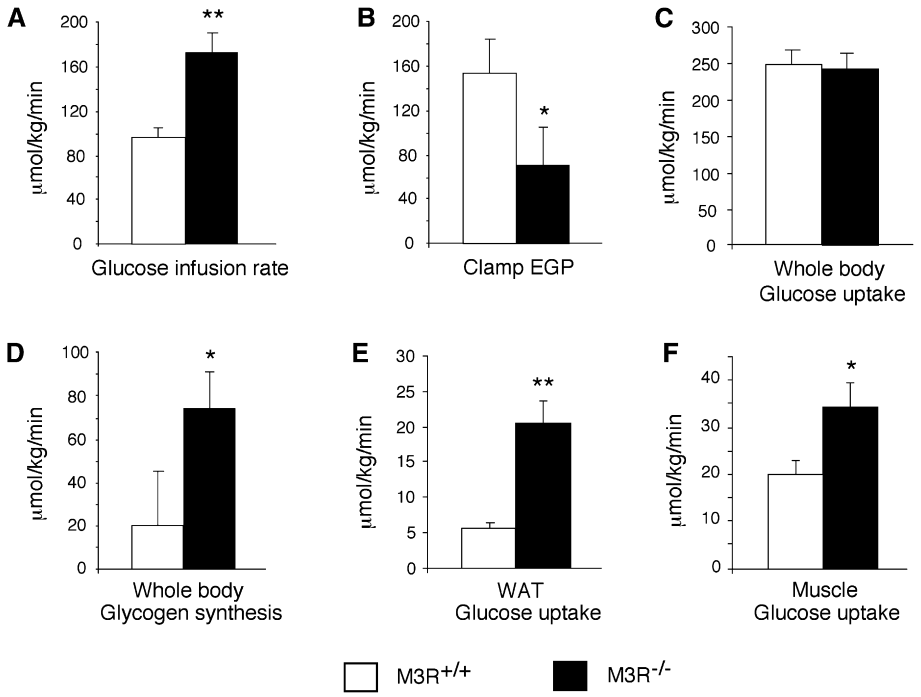

Figure 4. Analysis of $M3R^{+/+}$ and $M3R^{-/-}$ mice in euglycemic-hyperinsulinemic clamp studies

A–D) Whole-body glucose fluxes during euglycemic-hyperinsulinemic clamp studies (EGP, endogenous glucose production). **E)** Glucose uptake into white adipose tissue (WAT, epididymal fat) during clamp studies. **F)** Glucose uptake into skeletal muscle (gastrocnemius muscle) during clamp studies. Data are given as means ± SEM ($M3R^{+/+}$, n = 7; $M3R^{-/-}$, n = 8; 3-month-old males). *p < 0.05; **p < 0.01.

liver, fat, and skeletal muscle, tissues which play key roles in glucose and energy homeostasis. Specifically, we incubated cell membranes prepared from liver, white adipose tissue (WAT), brown adipose tissue (BAT), and gastrocnemius and triceps muscles from wild-type mice with a saturating concentration (3 nM) of the muscarinic radioligand, [^{3}H]quinuclidinyl benzilate ([^{3}H]QNB; this ligand labels M_3 as well as all other muscarinic receptor subtypes). However, no specific [^{3}H]QNB binding was detectable in liver, WAT, BAT, and skeletal muscle tissues (detection limit of the binding assay used: ~1–2 fmoles receptors/mg protein). Under the same experimental conditions, the number of specific [^{3}H]QNB binding sites present in brain membranes ($M3R^{+/+}$ mice) amounted to 1074 ± 82 fmol/mg (n = 3).

Real-time quantitative RT-PCR studies confirmed that M_3 receptor mRNA was abundantly expressed in the brains of wild-type mice (Figure S3). In contrast, only very low levels of M_3 receptor transcripts were found in liver, WAT, and skeletal muscle, and no M_3 receptor mRNA was detectable in BAT (Figure S3). Since M_3 receptors are present on peripheral vascular epithelia (Lamping et al., 2004) and peripheral nerve endings (Garcia et al., 2005), it remains unclear which specific cell types are responsible for the small number of M_3 receptor transcripts detectable in mouse liver, WAT, and skeletal muscle.

$M3R^{-/-}$ mice display increased insulin sensitivity in liver, skeletal muscle, and fat

In insulin tolerance tests, $M3R^{-/-}$ mice showed an increase in insulin sensitivity (Figures 1G, 2G, and 3G). To examine the insulin sensitivity of individual tissues, we carried out euglycemic-hyperinsulinemic clamp studies using $M3R^{+/+}$ and $M3R^{-/-}$ mice maintained on standard chow (3-month-old males). The glucose infusion rate was adjusted in order to maintain blood glucose levels in $M3R^{+/+}$ and $M3R^{-/-}$ mice at similar levels (~150 mg/dl). Insulin was infused at the rate of 2.5 mU/kg/min to maintain insulin levels within a physiological range ($M3R^{+/+}$, 1.73 ± 0.10 ng/ml, n = 7; $M3R^{-/-}$, 1.13 ± 0.10 ng/ml, n = 8). Although $M3R^{-/-}$ mice showed significantly lower insulin levels during the clamp ($p < 0.01$), the glucose infusion rate was nearly 2-fold higher in $M3R^{-/-}$ mice than in control littermates (Figure 4A), confirming that M_3 receptor ablation leads to increased insulin sensitivity. The higher glucose infusion rate displayed by the $M3R^{-/-}$ mice correlated with reduced endogenous glucose production (Figure 4B), suggesting that $M3R^{-/-}$ mice had increased insulin sensitivity in the liver. Although whole-body glucose uptake rate was comparable in both groups of mice under the experimental conditions used (Figure 4C), $M3R^{-/-}$ mice showed a significantly elevated rate of whole-body glycogen synthesis (Figure 4D) and tended to have a lower rate of glycolysis (data not shown). Furthermore, glucose uptake in WAT (epididymal fat; Figure 4E) and skeletal muscle (gastrocnemius muscle; Figure 4F) was increased by ~250% and ~75%, respectively. Glucose uptake was also increased in BAT of $M3R^{-/-}$ mice ($M3R^{+/+}$, 1550 ± 261 µmol/kg/min, n = 7; $M3R^{-/-}$, 2095 ± 221 µmol/kg/min, n = 8); however, this difference failed to reach statistical significance ($p = 0.066$). These data clearly indicate that the lack of M_3 receptors leads to increased insulin sensitivity in the three major insulin target tissues (liver, skeletal muscle, and fat).

Histological studies

As shown in Figure S4, adipocyte size (BAT and WAT) was greatly decreased in $M3R^{-/-}$ mice, as compared to $M3R^{+/+}$ littermates. Moreover, fat deposits in the liver were much smaller in $M3R^{-/-}$ than in $M3R^{+/+}$ mice (animals had free access to regular chow; Figure S4). All other organs and tissues appeared histologically normal.

Increased expression of UCP3 in skeletal muscle of $M3R^{-/-}$ mice

The uncoupling proteins UCP1, UCP2, and UCP3 are mitochondrial inner membrane proteins that uncouple the proton gradient from ATP synthesis (Boss et al., 2000; Argyropoulos and Harper,

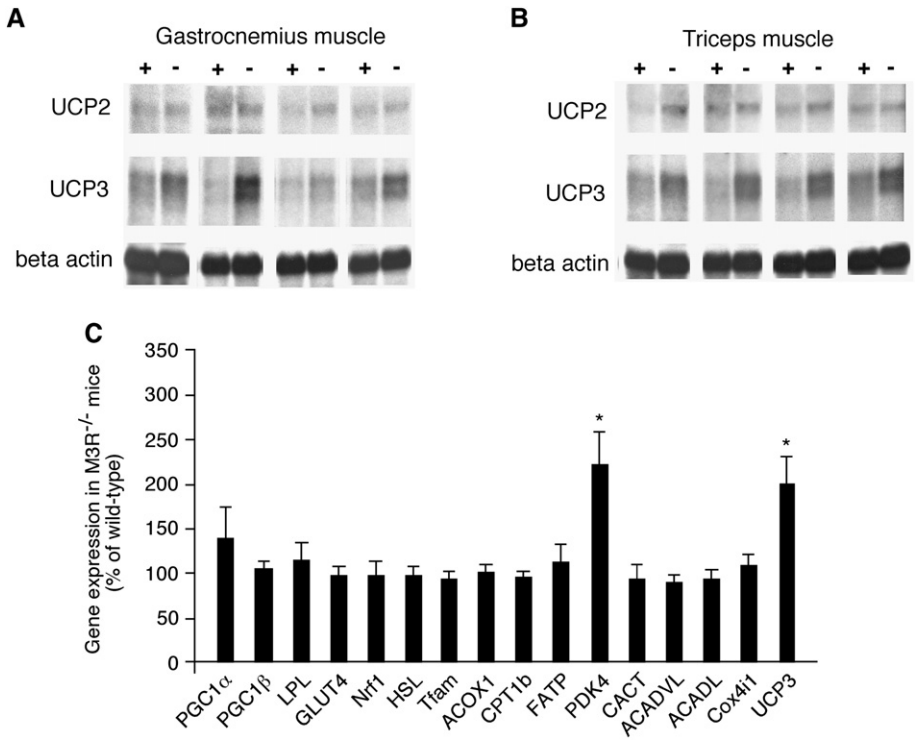

Figure 5. Gene expression in skeletal muscle of $M3R^{+/+}$ and $M3R^{-/-}$ mice

Northern blot analysis of UCP2 and UCP3 expression in gastrocnemius (**A**) and triceps (**B**) muscles of $M3R^{+/+}$ (+) and $M3R^{-/-}$ (–) mice (5-month-old males). Total RNA samples were electrophoresed (3 μg per lane), blotted, and probed for UCP2 and UCP3 expression. Each lane contains RNA obtained from a different mouse. Each blot was also hybridized with a β-actin probe as a loading control. **C)** Gene expression was studied by real-time quantitative PCR using total RNA prepared from gastrocnemius muscle of $M3R^{+/+}$ and $M3R^{-/-}$ mice (3-month-old males). Full gene names are provided in Table S3. Data were normalized relative to the expression of cyclophilin A, which served as an internal control. Results are presented as percent change in gene expression in $M3R^{-/-}$ mice as compared to wild-type littermates (n = 4 per group). *$p < 0.05$ versus wild-type.

2002; Rousset et al., 2004; Krauss et al., 2005). Several studies have shown that activation of the SNS and β-adrenergic receptor agonists can stimulate UCP expression in various tissues (Simonsen et al., 1992; Gong et al., 1997; Teshima et al., 1999; Boivin et al., 2000; Lowell and Spiegelman, 2000; Masaki et al., 2003). Given the increases in metabolic rate and SNS activity displayed by the $M3R^{-/-}$ mice, we examined whether UCP expression levels were altered in the absence of M_3 receptors. Specifically, we carried out Northern blotting experiments using tissues from $M3R^{+/+}$ and $M3R^{-/-}$ mice maintained on regular chow. We found that the lack of M_3 receptors had no significant effect on UCP1, UCP2, and UCP3 expression in BAT, UCP2 and UCP3 expression in WAT, and UCP2 expression in liver (data not shown). Likewise, real-time quantitative RT-PCR studies showed that UCP1 expression was similar in BAT of $M3R^{+/+}$ and $M3R^{-/-}$ mice (Figure S5). However, Northern blotting analysis indicated that transcript levels of UCP3, the predominant UCP expressed in skeletal muscle (Boss et al., 2000; Rousset et al., 2004; Krauss et al., 2005), were significantly higher in gastrocnemius and triceps muscles from $M3R^{-/-}$ mice (Figures 5A and 5B). Densitometric analysis of band intensities indicated that UCP3 expression levels in gastrocnemius and triceps muscle were increased by 73% ± 23% and 42% ± 3%, respectively, in $M3R^{-/-}$ mice (n = 4 per genotype and muscle). UCP2 expression levels were similar in skeletal muscle preparations from $M3R^{+/+}$ and $M3R^{-/-}$ mice (Figures 5A and 5B).

Increased expression of PDK4 in skeletal muscle of $M3R^{-/-}$ mice

Changes in the expression levels of UCPs are frequently associated with altered expression levels of other genes involved in the regulation of mitochondrial function and energy metabolism. We therefore used real-time quantitative RT-PCR to study the expression of various genes involved in regulating metabolic and mitochondrial functions in skeletal muscle (gastrocnemius muscle) from $M3R^{+/+}$ and $M3R^{-/-}$ mice (Figure 5C). The expression levels of most analyzed genes were not significantly affected by the lack of M_3 receptors. However, the RT-PCR studies confirmed that UCP3 expression was increased by approximately 2-fold in skeletal muscle from $M3R^{-/-}$ mice (Figure 5C). Moreover, PDK4 (pyruvate dehydrogenase kinase 4) expression was also ~2-fold higher in skeletal muscle tissue from $M3R^{-/-}$ mice (Figure 5C). PDK4 inactivates pyruvate dehydrogenase via phosphorylation, thus conserving 3-C compounds under conditions when glucose availability is limited and stimulating fatty-acid oxidation for the generation of ATP (Holness and Sugden, 2003).

In vivo fatty-acid oxidation

The data described above suggested that the lack of M_3 receptors might be associated with an increase in fatty-acid oxidation. To test this hypothesis, we measured in vivo fatty-acid oxidation in fasted $M3R^{+/+}$ and $M3R^{-/-}$ mice (3-month-old males). Specifically, we determined the rate of $^{14}CO_2$ production following i.p. injection of mice with [1-^{14}C] oleic acid (1 μCi). As shown in Figure 6, $M3R^{-/-}$ mice showed significant increases in in vivo fatty-acid oxidation after injection of [1-^{14}C] oleic acid. For example, when $^{14}CO_2$ production was expressed per g body weight (Figure 6A), the rate of fatty-acid oxidation was about 2-fold higher in $M3R^{-/-}$ than in $M3R^{+/+}$ mice.

Previous studies have shown that increased sympathetic tone stimulates fatty-acid oxidation in skeletal muscle via activation of α-adrenergic receptors (Minokoshi et al., 2002; Cha et al., 2005). To explore the possibility that the increase in in vivo fatty-acid oxidation displayed by the $M3R^{-/-}$ mice was mediated by stimulation of α-adrenergic receptors, we tested the effect of the α-receptor blocker phentolamine (10 mg/kg; i.p.) on in vivo fatty-acid oxidation in $M3R^{+/+}$ and $M3R^{-/-}$ mice

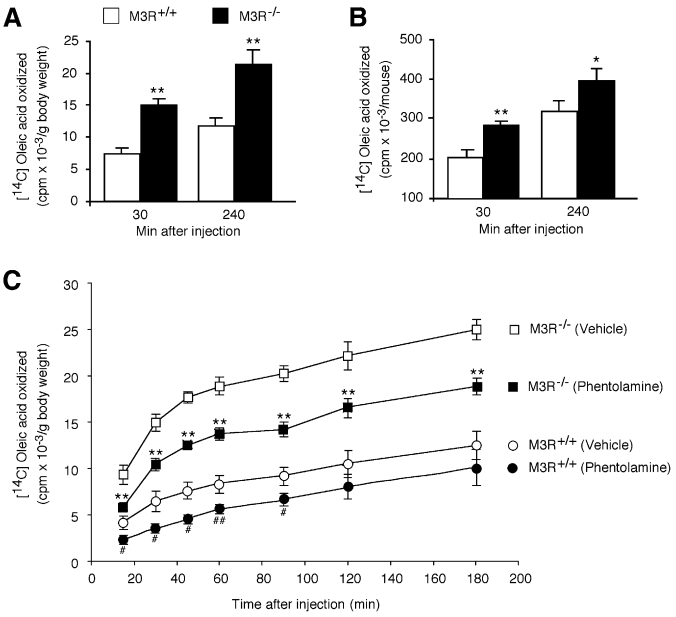

Figure 6. In vivo fatty-acid oxidation studies

After an overnight fast, $M3R^{+/+}$ and $M3R^{-/-}$ mice (3-month-old males), were injected i.p. with [1-^{14}C] oleic acid (1 μCi). The rate of $^{14}CO_2$ production was determined at the indicated time points, as described under Experimental Procedures. Results are presented as [1-^{14}C] oleic acid oxidized per g body weight (**A**) or per mouse (**B**). Data are given as means ± SEM (n = 8 per group). *$p < 0.05$; **$p < 0.01$. **C)** Fatty-acid oxidation was measured in fasted $M3R^{+/+}$ and $M3R^{-/-}$ mice (8.5-month-old males) following i.p. injection of [1-^{14}C] oleic acid (1 μCi) and the α-receptor blocker phentolamine (10 mg/kg) or saline (vehicle controls). Data are given as means ± SEM (n = 5 per group). **$p < 0.01$, as compared to the corresponding control group (vehicle, saline; $M3R^{-/-}$); $^{\#}p < 0.05$; $^{\#\#}p < 0.01$, as compared to the corresponding control group (vehicle, saline; $M3R^{+/+}$).

(8.5-month-old males). At all time points tested (Figure 6C), phentolamine treatment led to a drastic reduction (by ~50%) in fatty-acid oxidation in $M3R^{-/-}$ mice, as compared to saline-treated $M3R^{-/-}$ mice. In contrast, phentolamine treatment caused only a relatively small reduction in fatty-acid oxidation in $M3R^{+/+}$ mice, as compared to saline-treated $M3R^{+/+}$ mice (Figure 6C).

Discussion

In the present study, we demonstrated that the lack of M_3 muscarinic receptors greatly ameliorated impairments in glucose homeostasis and insulin sensitivity in three mouse models of obesity (obesity was induced by a high-fat diet, administration of GTG, or leptin deficiency; Figures 1–3). On the other hand, the effects of M_3 receptor ablation on overall adiposity were clearly less pronounced, particularly in the experiments involving the use of leptin-deficient mice (Figure 3C), suggesting that the beneficial metabolic effects associated with the lack of M_3 receptors cannot be solely due to reduced adiposity but that other factors (e.g., central mechanisms) may also directly influence peripheral glucose homeostasis (see discussion below).

Strikingly, in all three mouse models, the lack of M_3 receptors was associated with an increase in resting metabolic rate, hyperactivity, and elevated body temperature. It is likely that the resulting increase in energy expenditure represents a major factor contributing to the reduced body weight and adiposity and improved glucose homeostasis observed with the $M3R^{-/-}$ mice. Interestingly, these phenotypes (increase in metabolic rate, hyperactivity, and elevated body temperature) were not observed when the M_3 receptor mutation was present on a mixed mouse genetic background (C57BL/6J × 129SvEv; Yamada et al., 2001). In the present study, we used $M3R^{-/-}$ mice that had been backcrossed for 10 generations onto the C57BL/6NTac background. The altered phenotypes of $M3R^{-/-}$ mice revealed in the present study highlight the importance of studying the effects of gene deletions on a congenic or isogenic genetic background (Gerlai, 1996).

Consistent with previous results (Yamada et al., 2001), we observed that $M3R^{-/-}$ mice consumed significantly less food (regular chow or high-fat diet) than their wild-type littermates. We previously presented data suggesting that this hypophagia phenotype is due, at least partially, to the disruption of a central cholinergic pathway that stimulates food intake in wild-type mice via activation of hypothalamic M_3 receptors (Yamada et al., 2001). In the present study, we found that the lack of M_3 receptors was also able to prevent or greatly reduce the hyperphagia caused by GTG administration (Figure 2H) or by disruption of the leptin gene (Figure 3H), respectively. This reduction in calorie intake and the observed increase in energy expenditure are predicted to represent major factors responsible for the improvements in glucose homeostasis displayed by GTG-treated $M3R^{-/-}$ and $M3R^{-/-}$ *ob/ob* mice.

We noted that many of the phenotypic changes exhibited by the $M3R^{-/-}$ mice, including the observed increases in metabolic rate, locomotor activity, and body temperature, are consistent with an elevated tone of the sympathetic nervous system (SNS; Hoffman and Taylor, 2001). In agreement with this notion, we found that urine epinephrine and norepinephrine levels were significantly increased in $M3R^{-/-}$ mice. Although the precise mechanism underlying this increase in sympathetic outflow remains unclear at present, one possibility is that central (e.g., hypothalamic) M_3 receptors exert an inhibitory influence on sympathetic outflow in wild-type mice and that the lack of this inhibition in $M3R^{-/-}$ mice triggers the observed elevation in SNS activity. In agreement with this concept, central sympathetic outflow is known to be regulated by the activity of central cholinergic pathways (reviewed by Nonogaki, 2000).

Several studies have shown that increased SNS activity and adrenergic receptor agonists can stimulate the expression of UCPs (UCP1, UCP2, and/or UCP3) that have been shown to mediate mitochondrial proton leak in various tissues (Simonsen et al., 1992; Gong et al., 1997; Teshima et al., 1999; Boivin et al., 2000; Lowell and Spiegelman, 2000; Masaki et al., 2003; Krauss et al., 2005). We found that transcript levels of UCP3, the major UCP expressed in skeletal muscle (Boss et al., 2000; Rousset et al., 2004; Krauss et al., 2005), were significantly increased in skeletal muscle of $M3R^{-/-}$ mice (Figure 5). Skeletal muscle is known to be the most important contributor to basal metabolic rate and energy expenditure, partially due to proton leak in resting skeletal muscle (Zurlo et al., 1990; Rolfe and Brand, 1996; Rolfe and Brown, 1997). One possibility therefore is that increased SNS activity leads to a selective increase in UCP3 expression in skeletal muscle of $M3R^{-/-}$ mice, which in turn triggers increased energy expenditure, contributing to the reduction in body weight and obesity associated with the lack of M_3 receptors.

It has also been proposed that UCP3 may act as a mitochondrial fatty-acid efflux protein, thus stimulating fatty-acid

oxidation (Himms-Hagen and Harper, 2001; Argyropoulos and Harper, 2002). In agreement with this notion, we found that M3R$^{-/-}$ mice displayed a pronounced increase in the rate of fatty-acid oxidation in vivo (Figure 6). This elevated fatty-acid oxidation rate could be greatly reduced by treatment of M3R$^{-/-}$ mice with the α-receptor blocker phentolamine (Figure 6C), indicating that increased sympathetic tone makes a major contribution to this phenotype. Consistent with our findings, previous studies have shown that increased sympathetic tone stimulates fatty-acid oxidation in skeletal muscle via activation of α-adrenergic receptors (Minokoshi et al., 2002; Cha et al., 2005).

It should be noted, however, that UCP3 mRNA levels are usually elevated in states associated with increased fat metabolism (Boss et al., 2000; Argyropoulos and Harper, 2002; Krauss et al., 2005). We therefore cannot exclude the possibility that the observed increase in UCP3 expression in skeletal muscle of M3R$^{-/-}$ mice is secondary to the enhanced fatty-acid oxidation rate displayed by these mutant mice.

Quantitative RT-PCR studies showed that the expression of PDK4 was also upregulated in skeletal muscle from M3R$^{-/-}$ mice (Figure 5C). PDK4 inactivates pyruvate dehydrogenase via phosphorylation, thus conserving 3-C compounds under conditions when glucose availability is limited and stimulating fatty-acid oxidation for the generation of ATP (Holness and Sugden, 2003). Because of the large contribution of skeletal muscle to whole-body glucose disposal, suppression of pyruvate dehydrogenase by PDK4 in skeletal muscle is likely to be of particular relevance for glucose homeostasis (Holness and Sugden, 2003). Our data are therefore consistent with the concept that the lack of M_3 receptors leads to a relative shortage of glucose, resulting in increased expression of PDK4 in skeletal muscle, reduced oxidative breakdown of glucose, and increased mitochondrial fatty-acid oxidation to ensure proper ATP production.

As discussed above, several lines of evidence suggest that the lack of M_3 receptors leads to increased central sympathetic outflow. Increased activity of the SNS usually leads to increased expression of UCP1 in BAT (Lowell and Spiegelman, 2000). Although adipocyte size was greatly decreased in BAT of M3R$^{-/-}$ mice (compared to M3R$^{+/+}$ littermates; Figure S4), Northern blotting studies (data not shown) and real-time quantitative RT-PCR analysis (Figure S5) showed that UCP1 expression was similar in BAT of M3R$^{+/+}$ and M3R$^{-/-}$ mice. At present, we do not have a clear explanation for the observation that UCP1 expression remains unchanged in BAT of M3R$^{-/-}$ mice despite increased SNS activity. One possibility is that other as yet unknown factors or pathways that are affected by the lack of M_3 receptors counteract the increase in UCP1 expression in BAT that is usually associated with increased sympathetic outflow.

Under all experimental conditions used in the present study, the absence of M_3 receptors was associated with a striking increase in insulin sensitivity. Euglycemic-hyperinsulinemic clamp studies demonstrated that deletion of the M_3 receptor gene led to a pronounced stimulation of glucose uptake in skeletal muscle and WAT (Figure 4). Radioligand binding studies indicated that skeletal muscle and WAT preparations from wild-type mice did not express detectable levels of M_3 or other muscarinic receptors, excluding the possibility that the increase in insulin sensitivity displayed by the M3R$^{-/-}$ mice is due to the lack of M_3 receptors in these tissues. Since M3R$^{-/-}$ *ob/ob* mutant mice showed only a rather small reduction in adiposity (as compared to *ob/ob* mice) but displayed greatly improved glucose tolerance and insulin sensitivity (Figure 3), it is likely that factors unrelated to overall adiposity, probably involving central cholinergic pathways, also contribute to the beneficial metabolic effects associated with the absence of M_3 receptors.

Whereas our data strongly suggest that activation of M_3 muscarinic acetylcholine receptors promotes adiposity (at least in the case of diet-induced obesity), administration of the classic nicotinic acetylcholine receptor agonist, nicotine, inhibits food intake, increases metabolic rate, and leads to reduced adiposity (Li et al., 2003). There are several other examples where stimulation of muscarinic and nicotinic acetylcholine receptors results in opposing physiological or behavioral responses. For instance, while nicotine exerts antidepressant-like effects and usually leads to locomotor stimulation (Picciotto et al., 2000), administration of centrally active muscarinic agonists causes depressogenic effects and reduced locomotor activity (Bymaster and Felder, 2002; Wess, 2004). It is likely that the existence of multiple nicotinic and muscarinic receptor subtypes and the different anatomical distributions of these receptor subtypes are major factors responsible for these opposing effects. It should also be noted that nicotine administration (smoking) promotes glucose intolerance, insulin resistance, and type 2 diabetes, involving various sites and mechanisms of action (Kapoor and Jones, 2005).

In conclusion, the lack of M_3 receptors has pronounced effects on energy and glucose homeostasis in mice. M3R$^{-/-}$ mice are largely protected against the detrimental metabolic deficits triggered by a high-fat diet, chemical disruption of ventromedial hypothalamic neurons by GTG, and genetic disruption of the leptin gene. The M_3 receptor may therefore represent a potential pharmacologic target for the treatment of obesity and associated metabolic disorders. However, since peripheral M_3 receptors are known to play a key role in mediating acetylcholine-induced glandular secretion and smooth muscle contractions (Eglen et al., 1996; Caulfield and Birdsall, 1998; Wess, 2004), the potential therapeutic use of M_3 receptor antagonists may cause significant peripheral side effects. It is possible that such side effects can be minimized by administration of antagonist doses that do not block M_3 receptor function completely or by the use of lipophilic M_3 receptor antagonists that accumulate in the brain.

Experimental procedures

Animals

The generation of M3R$^{-/-}$ mice has been described previously (Yamada et al., 2001). M3R$^{-/-}$ mice were backcrossed for 10 generations onto the C57BL/6NTac background (Taconic Farms, Germantown, New York). All mice used in the present study were male littermates resulting from heterozygous matings. To generate *ob/ob* mice lacking the M_3 receptor gene, M3R$^{-/-}$ males were first bred to *ob*/+ females (C57BL/6J background; The Jackson Laboratory, Bar Harbor, Maine) to obtain compound heterozygotes (M3R$^{+/-}$ *ob*/+). These compound heterozygotes were then interbred to generate M3R$^{-/-}$ *ob/ob*, *ob/ob*, M3R$^{-/-}$, and M3R$^{+/+}$ mice (wild-type littermates). Genotypes were confirmed by PCR amplification of genomic DNA (primer sequences are available upon request).

All animal studies were approved by the Animal Care and Use Committee of the National Institute of Diabetes and Digestive and Kidney Diseases, National Institutes of Health, Bethesda, Maryland.

Mouse maintenance and food intake studies

Mice were housed four to five per cage in a specific pathogen-free barrier facility, maintained on a 12 hr light/dark cycle. Unless indicated otherwise,

all experiments were carried out with male littermates that were 3–6 months old at the time of testing.

Mice were fed ad libitum with a standard mouse chow (5% [w/w] fat content; 4.08 kcal/g; Zeigler, Gardners, Pennsylvania). For diet-induced obesity studies, 4-week-old male mice were put on a high-fat diet (35.5% [w/w] fat content; 5.45 kcal/g; # F3282, Bioserv, Frenchtown, New Jersey) for 16 weeks. Obesity was also induced chemically by injecting 4-week-old male mice with a single dose of GTG (0.5 mg/g, i.p.).

For food intake studies, mice were individually housed and fed ad libitum. The food intake data shown in Figure 1H were obtained by using special tunnel-type feeders (Rodent Cafe Type-M; OYC International, Inc.). Food was weighed daily for 6 days.

Glucose and insulin tolerance tests

For glucose and insulin tolerance tests, mice that had been subjected to an overnight (10–12 hr) fast were given i.p. glucose (2 mg/g body weight) or insulin (Humulin, 0.75 mIU/g; Eli Lilly), respectively. Tail blood was collected before (time 0) and at indicated times after injection of glucose or insulin for the measurement of glucose (Glucometer Elite; Bayer).

Biochemical assays

Serum insulin and plasma leptin concentrations were determined via ELISA (Crystal Chem Inc.). Serum T3 and T4 levels were measured via RIA (Diagnostic Products). Serum-free fatty acids were determined via colorimetry using a kit purchased from Roche Diagnostics Corp.

Body composition, metabolic rate, locomotor activity, and body temperature measurements

Body composition was measured using the NMR analyzer Bruker Minispec mq10 (Bruker Optics Inc.). O_2 consumption, CO_2 release rates, and locomotor activity levels were determined at room temperature using the Oxymax system (Columbus Instruments, Ohio), as described previously (Yu et al., 2000). Body temperature measurements were taken between 1 and 3 pm or at midnight using a rectal thermometer (model TH-5; Braintree Scientific, Massachusetts).

Fat absorption studies and charcoal transit test

The high-fat diet used for fat absorption studies was composed as follows (percentage weight): 35.5% fat (safflower oil), 50% nonfat dry milk, and 14.5% sucrose, providing 55:31:14 fat:protein:carbohydrate energy percentage. The fat component contained 5% weight sucrose polybehenate (olestra), which is not hydrolyzed by pancreatic lipase and not absorbed from the intestine. Fecal samples were collected from mice that had been fed the high-fat diet for 3 days. Percent fat absorption was determined by comparing the known ratio of fat (triacylglycerol) to marker in the diet and the measured ratio of fat (all forms of fatty acids: fatty acids, monoacylglycerols, diacyglycerols, and triacylglycerols) to marker in the feces, as described in detail by Jandacek et al. (2004). A charcoal transit test was used to measure gastrointestinal motor function in vivo, as described in detail previously (Yamada et al., 2001).

Determination of urine catecholamines

Urine samples were collected over a 24 hr period using mice housed in metabolic cages (2 mice per cage). Urine epinephrine and norepinephrine were quantified by HPLC (Eisenhofer et al., 1986; measured by Ani Lytics Inc.).

Radioligand binding studies

Membranes prepared from different mouse tissues (liver, BAT, WAT, and gastrocnemius and triceps muscles) were incubated with a saturating concentration (3 nM) of the non-subtype-selective muscarinic antagonist, [^{3}H]QNB (42 Ci/mmol; PerkinElmer), essentially as described (Dörje et al., 1991). Binding reactions were carried out for 1 hr at room temperature (22°C). Nonspecific binding was determined in the presence of 10 μM atropine.

Hyperinsulinemic-euglycemic clamp studies

Hyperinsulinemic-euglycemic clamp studies and in vivo glucose flux analysis were carried out as previously described (Pennisi et al., 2006).

In vivo fatty-acid oxidation

Fatty-acid ([1-^{14}C] oleic acid) oxidation was measured in vivo using a method similar to that described by Cha et al. (2005). Mice were fasted overnight, injected with [1-^{14}C] oleic acid (Perkin Elmer NEC317, 1 μCi in 200 μl of saline i.p.), and placed into a sealed chamber connected to an air pump (Thomas Scientific # 7893B05) and a 50 ml tube containing 3 M NaOH solution to trap expired $^{14}CO_2$. One milliliter aliquots were taken 30 and 240 min after injection of [1-^{14}C] oleic acid to calculate the oxidation of [1-^{14}C] oleic acid to $^{14}CO_2$.

Northern analysis

Total RNA was prepared from different tissues of M3R$^{+/+}$ and M3R$^{-/-}$ mice using the RNeasy fibrous tissue kit (Qiagen, Valencia, California) according to the manufacturer's instructions. Three micrograms of total RNA was analyzed by Northern blotting according to standard techniques using ^{32}P-labeled probes. The UCP1 and UCP3 probes were identical to the ones used by Gong et al. (1997). The UCP2 probe used in the present study has been described by McPherron and Lee (2002). Band intensities were measured via densitometry using ImageJ (NIH) and were normalized relative to β-actin expression.

Real-time quantitative RT-PCR

Total RNA was isolated from mouse skeletal muscle (gastrocnemius muscle) using the RNeasy fibrous tissue kit (Qiagen) and treated with DNase I for 15 min at room temperature. RNA integrity was confirmed by using the Agilent 2100 Bioanalyzer (Agilent Technologies). Reverse transcription was performed using MultiScribe RT (Applied Biosystems), and gene expression levels were measured by real-time quantitative RT-PCR (7900HT SDS; Applied Biosystems). PCR reactions (25 μl total volume) included cDNA (~10 ng of initial RNA sample), 100–120 nM of each primer, and 12.5 μl of 2× SYBR Green Master Mix (Applied Biosystems). The PCR cycling conditions were as follows: 50°C for 2 min, 95°C for 10 min, and 40 cycles at 95°C for 15 s, and 60°C for 1 min, respectively. The specificity of each RT-PCR product was checked via gel electrophoresis. The expression of cyclophilin A served as an internal control. Four independent samples prepared from four different mice were used per genotype. PCR reactions were carried out in triplicate. The results were expressed as percent change in gene expression relative to cyclophilin A expression between M3R$^{+/+}$ and M3R$^{-/-}$ mice. Primer sequences are provided in Table S3.

Morphological studies

Mouse tissues were fixed in 10% neutral buffered formalin, processed into paraffin blocks, sectioned at 6 microns, and stained with hematoxylin and eosin. Stained sections were examined by light microscopy (Olympus BX41). Photographs were taken with an Olympus DP12 digital camera, using the 20× oil immersion lens.

Statistics

Data are expressed as means ± SEM for the indicated number of observations. Statistical significance between groups was determined using two-tailed Student's t test or one-way analysis of variance followed by appropriate post-hoc tests.

Supplemental data

Supplemental data include three tables and five figures and can be found with the article online at http://www.cellmetabolism.org/cgi/content/4/5/363/DC1/.

Acknowledgments

This work was supported by the Intramural Research Program, NIDDK, NIH, US Department of Health and Human Services. We thank Dr. Ronald J. Jandacek from the University of Cincinnati (Ohio) for carrying out the fat absorption studies, Dr. Se-Jin Lee for kindly providing the UCP2 probe, Dr. Lee Weinstein for providing the sequences of several RT-PCR primers, Dr. Georgina Miller for help with the histological analysis of mouse tissues, and Drs. Kevin Hall and Juen Guo for advice and helpful discussions.

Received: April 20, 2006
Revised: September 6, 2006
Accepted: September 26, 2006
Published: November 7, 2006

References

Ahren, B. (2000). Autonomic regulation of islet hormone secretion–implications for health and disease. Diabetologia *43*, 393–410.

Argyropoulos, G., and Harper, M.E. (2002). Uncoupling proteins and thermoregulation. J. Appl. Physiol. *92*, 2187–2198.

Bergen, H.T., Mizuno, T.M., Taylor, J., and Mobbs, C.V. (1998). Hyperphagia and weight gain after gold-thioglucose: relation to hypothalamic neuropeptide Y and proopiomelanocortin. Endocrinology *139*, 4483–4488.

Boivin, M., Camirand, A., Carli, F., Hoffer, L.J., and Silva, J.E. (2000). Uncoupling protein-2 and -3 messenger ribonucleic acids in adipose tissue and skeletal muscle of healthy males: variability, factors affecting expression, and relation to measures of metabolic rate. J. Clin. Endocrinol. Metab. *85*, 1975–1983.

Boss, O., Hagen, T., and Lowell, B.B. (2000). Uncoupling proteins 2 and 3: potential regulators of mitochondrial energy metabolism. Diabetes *49*, 143–156.

Bray, G.A., and York, D.A. (1979). Hypothalamic and genetic obesity in experimental animals: an autonomic and endocrine hypothesis. Physiol. Rev. *59*, 719–809.

Bymaster, F.P., and Felder, C.C. (2002). Role of the cholinergic muscarinic system in bipolar disorder and related mechanism of action of antipsychotic agents. Mol. Psychiatry *7* (*Suppl. 1*), S57–S63.

Caulfield, M.P., and Birdsall, N.J.M. (1998). International Union of Pharmacology. XVII. Classification of muscarinic acetylcholine receptors. Pharmacol. Rev. *50*, 279–290.

Cha, S.H., Hu, Z., Chohnan, S., and Lane, M.D. (2005). Inhibition of hypothalamic fatty acid synthase triggers rapid activation of fatty acid oxidation in skeletal muscle. Proc. Natl. Acad. Sci. USA *102*, 14557–14562.

Dörje, F., Wess, J., Lambrecht, G., Tacke, R., Mutschler, E., and Brann, M.R. (1991). Antagonist binding profiles of five cloned human muscarinic receptor subtypes. J. Pharmacol. Exp. Ther. *256*, 727–733.

Duttaroy, A., Zimliki, C.L., Gautam, D., Cui, Y., Mears, D., and Wess, J. (2004). Muscarinic stimulation of pancreatic insulin and glucagon release is abolished in M_3 muscarinic acetylcholine receptor-deficient mice. Diabetes *53*, 1714–1720.

Eglen, R.M., Hegde, S.S., and Watson, N. (1996). Muscarinic receptor subtypes and smooth muscle function. Pharmacol. Rev. *48*, 531–565.

Eisenhofer, G., Goldstein, D.S., Stull, R., Keiser, H.R., Sunderland, T., Murphy, D.L., and Kopin, I.J. (1986). Simultaneous liquidchromatographic determination of 3,4-dihydroxyphenylglycol, catecholamines, and 3,4-dihydroxyphenylalanine in plasma, and their responses to inhibition of monoamine oxidase. Clin. Chem. *32*, 2030–2033.

Garcia, N., Santafe, M.M., Salon, I., Lanuza, M.A., and Tomas, J. (2005). Expression of muscarinic acetylcholine receptors (M1-, M2-, M3- and M4-type) in the neuromuscular junction of the newborn and adult rat. Histol. Histopathol. *20*, 733–743.

Gerlai, R. (1996). Gene-targeting studies of mammalian behavior: is it the mutation or the background genotype? Trends Neurosci. *19*, 177–181.

Gilon, P., and Henquin, J.C. (2001). Mechanisms and physiological significance of the cholinergic control of pancreatic β-cell function. Endocr. Rev. *22*, 565–604.

Gong, D.W., He, Y., Karas, M., and Reitman, M. (1997). Uncoupling protein-3 is a mediator of thermogenesis regulated by thyroid hormone, β3-adrenergic agonists, and leptin. J. Biol. Chem. *272*, 24129–24132.

Himms-Hagen, J., and Harper, M.E. (2001). Physiological role of UCP3 may be export of fatty acids from mitochondria when fatty acid oxidation predominates: an hypothesis. Exp. Biol. Med. (Maywood) *226*, 78–84.

Hoffman, B.B., and Taylor, P. (2001). The autonomic and somatic motor nervous systems. In Goodman & Gilman's: The Pharmacological Basis of Therapeutics 10th edition, J.G. Hardman, L.E. Limbird, and A.G. Gilman, eds. (New York: McGraw-Hill), pp. 115–153.

Holness, M.J., and Sugden, M.C. (2003). Regulation of pyruvate dehydrogenase complex activity by reversible phosphorylation. Biochem. Soc. Trans. *31*, 1143–1151.

Jandacek, R.J., Heubi, J.E., and Tso, P. (2004). A novel, noninvasive method for the measurement of intestinal fat absorption. Gastroenterology *127*, 139–144.

Kapoor, D., and Jones, T.H. (2005). Smoking and hormones in health and endocrine disorders. Eur. J. Endocrinol. *152*, 491–499.

Krauss, S., Zhang, C.Y., and Lowell, B.B. (2005). The mitochondrial uncoupling-protein homologues. Nat. Rev. Mol. Cell Biol. *6*, 248–261.

Lam, T.K., Pocai, A., Gutierrez-Juarez, R., Obici, S., Bryan, J., Aguilar-Bryan, L., Schwartz, G.J., and Rossetti, L. (2005). Hypothalamic sensing of circulating fatty acids is required for glucose homeostasis. Nat. Med. *11*, 320–327.

Lamping, K.G., Wess, J., Cui, Y., Nuno, D.W., and Faraci, F.M. (2004). Muscarinic (M) receptors in coronary circulation: gene-targeted mice define the role of M_2 and M_3 receptors in response to acetylcholine. Arterioscler. Thromb. Vasc. Biol. *24*, 1253–1258.

Levey, A.I., Edmunds, S.M., Heilman, C.J., Desmond, T.J., and Frey, K.A. (1994). Localization of muscarinic m3 receptor protein and M3 receptor binding in rat brain. Neuroscience *63*, 207–221.

Li, M.D., Kane, J.K., and Konu, O. (2003). Nicotine, body weight and potential implications in the treatment of obesity. Curr. Top. Med. Chem. *3*, 899–919.

Lowell, B.B., and Spiegelman, B.M. (2000). Towards a molecular understanding of adaptive thermogenesis. Nature *404*, 652–660.

Masaki, T., Chiba, S., Yasuda, T., Tsubone, T., Kakuma, T., Shimomura, I., Funahashi, T., Matsuzawa, Y., and Yoshimatsu, H. (2003). Peripheral, but not central, administration of adiponectin reduces visceral adiposity and upregulates the expression of uncoupling protein in agouti yellow (A^y/a) obese mice. Diabetes *52*, 2266–2273.

McPherron, A.C., and Lee, S.J. (2002). Suppression of body fat accumulation in myostatin-deficient mice. J. Clin. Invest. *109*, 595–601.

Minokoshi, Y., Kim, Y.B., Peroni, O.D., Fryer, L.G., Müller, C., Carling, D., and Kahn, B.B. (2002). Leptin stimulates fatty-acid oxidation by activating AMP-activated protein kinase. Nature *415*, 339–343.

Niijima, A. (1989). Neural mechanisms in the control of blood glucose concentration. J. Nutr. *119*, 833–840.

Nonogaki, K. (2000). New insights into sympathetic regulation of glucose and fat metabolism. Diabetologia *43*, 533–549.

Pennisi, P., Gavrilova, O., Setser-Portas, J., Jou, W., Santopietro, S., Clemmons, D., Yakar, S., and Leroith, D. (2006). Recombinant human insulin-like growth factor-I (rhigf-1) treatment inhibits gluconeogenesis in a transgenic mouse model of type 2 Diabetes Mellitus (DM). Endocrinology *147*, 2619–2630.

Picciotto, M.R., Caldarone, B.J., King, S.L., and Zachariou, V. (2000). Nicotinic receptors in the brain. Links between molecular biology and behavior. Neuropsychopharmacology *22*, 451–465.

Röhl, M., Pasparakis, M., Baudler, S., Baumgartl, J., Gautam, D., Huth, M., De Lorenzi, R., Krone, W., Rajewsky, K., and Brüning, J.C. (2004). Conditional disruption of IκB kinase 2 fails to prevent obesity-induced insulin resistance. J. Clin. Invest. *113*, 474–481.

Rohner-Jeanrenaud, F. (1995). A neuroendocrine reappraisal of the dual-centre hypothesis: its implications for obesity and insulin resistance. Int. J. Obes. Relat. Metab. Disord. *19*, 517–534.

Rolfe, D.F., and Brand, M.D. (1996). Contribution of mitochondrial proton leak to skeletal muscle respiration and to standard metabolic rate. Am. J. Physiol. *271*, C1380–C1389.

Rolfe, D.F., and Brown, G.C. (1997). Cellular energy utilization and molecular origin of standard metabolic rate in mammals. Physiol. Rev. *77*, 731–758.

Rousset, S., Alves-Guerra, M.C., Mozo, J., Miroux, B., Cassard-Doulcier, A.M., Bouillaud, F., and Ricquier, D. (2004). The biology of mitochondrial uncoupling proteins. Diabetes *53* (*Suppl 1*), S130–S135.

Schwartz, M.W., Woods, S.C., Porte, D., Jr., Seeley, R.J., and Baskin, D.G. (2000). Central nervous system control of food intake. Nature *404*, 661–671.

Simonsen, L., Bülow, J., Madsen, J., and Christensen, N.J. (1992). Thermogenic response to epinephrine in the forearm and abdominal subcutaneous adipose tissue. Am. J. Physiol. *263*, E850–E855.

Teshima, Y., Saikawa, T., Yonemochi, H., Hidaka, S., Yoshimatsu, H., and Sakata, T. (1999). Alteration of heart uncoupling protein-2 mRNA regulated by sympathetic nerve and triiodothyronine during postnatal period in rats. Biochim. Biophys. Acta *1448*, 409–415.

Wess, J. (1996). Molecular biology of muscarinic acetylcholine receptors. Crit. Rev. Neurobiol. *10*, 69–99.

Wess, J. (2004). Muscarinic acetylcholine receptor knockout mice: novel phenotypes and clinical implications. Annu. Rev. Pharmacol. Toxicol. *44*, 423–450.

Yach, D., Stuckler, D., and Brownell, K.D. (2006). Epidemiologic and economic consequences of the global epidemics of obesity and diabetes. Nat. Med. *12*, 62–66.

Yamada, M., Miyakawa, T., Duttaroy, A., Yamanaka, A., Moriguchi, T., Makita, R., Ogawa, M., Chou, C.J., Xia, B., Crawley, J.N., et al. (2001). Mice lacking the M3 muscarinic acetylcholine receptor are hypophagic and lean. Nature *410*, 207–212.

Yu, S., Gavrilova, O., Chen, H., Lee, R., Liu, J., Pacak, K., Parlow, A.F., Quon, M.J., Reitman, M.L., and Weinstein, L.S. (2000). Paternal versus maternal transmission of a stimulatory G protein α subunit knockout produces opposite effects on energy metabolism. J. Clin. Invest. *105*, 615–623.

Zurlo, F., Larson, K., Bogardus, C., and Ravussin, E. (1990). Skeletal muscle metabolism is a major determinant of resting energy expenditure. J. Clin. Invest. *86*, 1423–1427.